Opto-Electronic Advances

Supplementary information

November 2024, Vol. 7, No. 11

DOI: 10.29026/oea.2024.240082

High-precision multi-focus laser sculpting of microstructured glass

Kang Xu[1,2†], Peilin Huang[1,2†], Lingyu Huang[2], Li Yao[2], Zongyao Li[2], Jiantao Chen[2], Li Zhang[3] and Shaolin Xu[2*]

[1]Department of Mechanical and Energy Engineering, Southern University of Science and Technology, 1088 Xueyuan Avenue, Shenzhen 518055, China; [2]Guangdong Provincial Engineering and Technology Research Center for Ultrafast Laser Micro-Nano Manufacturing Equipment and Technology, Shenzhen Guihua Intelligent Technology Co., Ltd., Dalang Avenue, Shenzhen 518109, China.

[†]These authors contributed equally to this work.

*Correspondence: SL Xu, Email: xusl@sustech.edu.cn

This file includes:

Section 1: Calculation and correction for phase diagram

Section 2: Experiments for corrections

Section 3: Morphology of glass grooves

Section 4: Fabrication parameters for each experiments

Supplementary information for this paper is available at https://doi.org/10.29026/oea.2024.240082

Section 1: Calculation and correction for phase diagram

The phase diagram for arbitrary multi-focus spot comes from the superposition of Gratings and Lenses following the equations below with corresponding coordinates in Fig. 2(a) and further adjustment.

Classical equation without any correction:

1) The target multi-focus coordinate on a line:

$$\boldsymbol{D}_j^0 = \boldsymbol{D}_j^0\left(x_j, y_j, z_j\right) \ , \tag{S1}$$

where the j is the sequence number of the point.

2) Derivation of grating period $p_{x,j}$ from x-direction distance which is the same as y-direction distance:

$$p_{x,j}\sin\theta = \lambda \ , \tag{S2}$$

$$\tan\theta = \frac{x_j}{f_{\mathrm{OB}}} \ , \tag{S3}$$

where λ is the laser wavelength and f_{OB} is the focal length of the objective.

3) Approximate derivation of Fresnel lens' focal length from z-direction distance:

$$\frac{1}{f_{\mathrm{OB}} + z_j} \approx \frac{1}{f_{0,j}} + \frac{1}{f_{\mathrm{OB}}} \ , \tag{S4}$$

where the z_j is coordinate of z, the f_0 is the focal length of Fresnel lens for light modulation.

4) The converted corresponding axis of the target foci for phase diagrams:

$$D_j^{\mathrm{phase}} = D_j^{\mathrm{phase}}\left(p_{x,j}, p_{y,j}, f_{0,j}\right) \ . \tag{S5}$$

Correction of the derivation equations:

1) Correction 1: To improve the uniformity, slight randomization for coordinate is introduced which is still on the target line as shown in Fig. 3(b):

$$\boldsymbol{D}_j^{\mathrm{random}} = \boldsymbol{D}_j^{\mathrm{random}}\left(x_j, y_j, z_j\right) \ . \tag{S6}$$

For example, we have a line with three dots: (1, 0, 1), (2, 0, 2), (3, 0, 3), (4, 0, 4), which follow the equation $z = x$. The randomization can be (1, 0, 1), (1.92, 0, 1.92), (2.95, 0, 2.95), (4, 0, 4). It is noticed that the terminal points remain unchanged to keep the length intact. The coordinates always have an offset less than 10% of the interval distance between adjacent points that is "$\sqrt{2}$" in this example. The practical selection of this ratio depends on the concrete design.

2) Correction 2 (Fig. S1): Adjustment of z-direction coordinate with error due to refractive index of glass n:

$$z_{0,j} = \frac{z_j}{n} \ , \tag{S7}$$

where z_j is the target coordinate, $z_{0,j}$is the optimized coordinate.

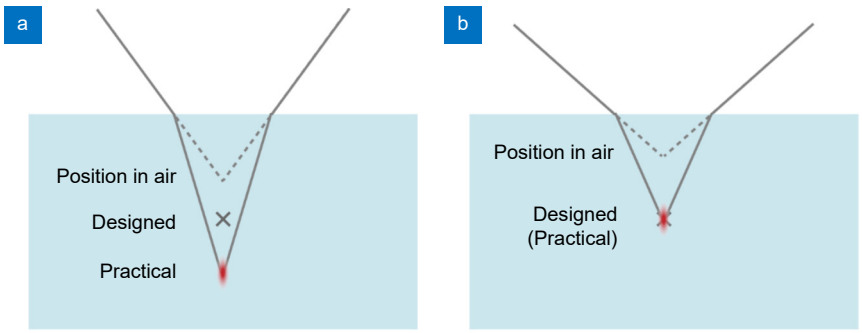

Fig. S1 | Schematic of z-direction axis (**a**) without and (**b**) with adjustment.

3) Correction 3 (Fig. S2): The refractive index and optimized focal distance are introduced into the grating derivation, where the zero point is not much far from the surface related to objective focal length by default:

$$p_{x,j}\sin\theta = \lambda \ , \tag{S8}$$

$$\tan\theta = \frac{x_j}{f_{\mathrm{OB}} + z_j} \ , \tag{S9}$$

where $p_{x,j}$ is the period of blaze grating, θ is deviation angle.

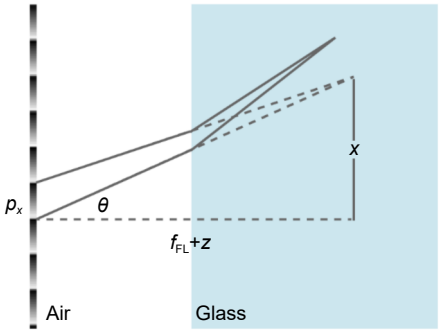

Fig. S2 | Schematic of optimization of *x*-direction axis that is as the same as *y*-direction axis.

4) Correction 4 (Fig. S3): The optimized relationship between propagation direction axis z and Fresnel lens focal length f_0 where the focal points of Fresnel lens and objectives do not overlap:

$$\frac{1}{f_{\mathrm{OB}} + z_{0,j}} = \frac{1}{f_{0,j}} + \frac{1}{f_{\mathrm{OB}}} - \frac{d}{f_{0,j} f_{\mathrm{OB}}} \ , \tag{S10}$$

where d is the distance between the phase diagram and the objective, which is constant for the certain optical system.

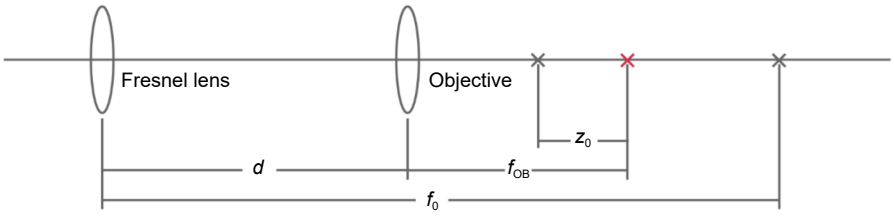

Fig. S3 | Schematic of practical condition for *z*-direction displacement.

5) The final parameters for foci:

$$D_j^{\mathrm{final}} = D_j^{\mathrm{final}}\left(p_{x,j}, p_{y,j}, f_{0,j}\right) \ , \tag{S11}$$

6) The final transmission function for phase image where the intensity is adjusted by introducing the normalized energy adjustment coefficient I:

$$T = Ae^{\phi i} = \sum_j \left[I_j \times \exp\left(\frac{2\pi r_x}{p_{x,j}} + \frac{2\pi r_y}{p_{y,j}} + \frac{\pi r_0^2}{\lambda f_{0,j}} \right) i \right] \ .$$

Section 2: Experiments for corrections

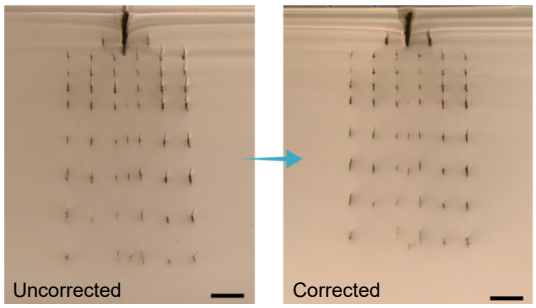

Fig. S4 | Correction of coordinate under irradiation by objective 20×. Scale bar: 100 μm.

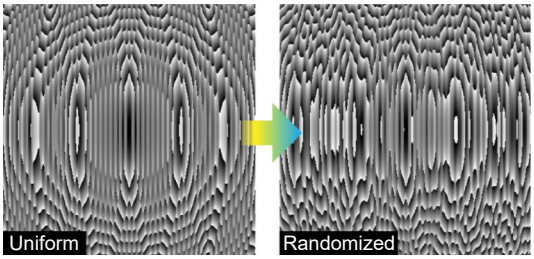

Fig. S5 | Change of phase diagram for V-shape dot array with 21 points when introducing randomization.

Section 3: Morphology of glass grooves

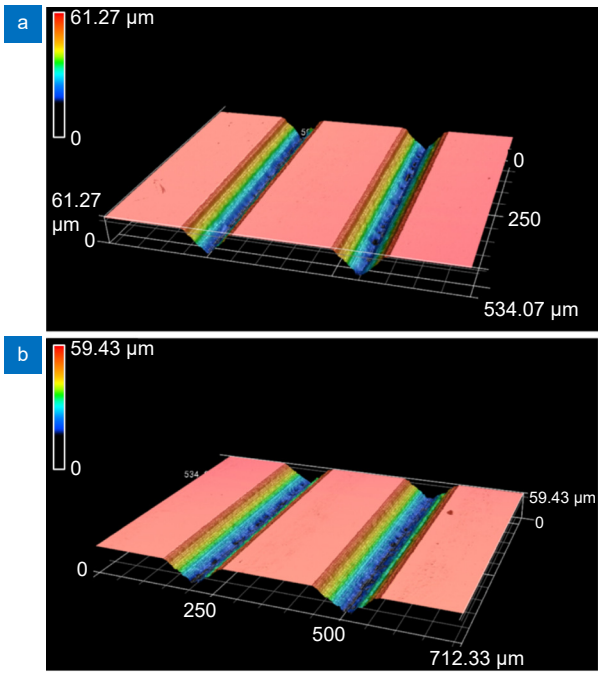

Fig. S6 | Morphology of isosceles triangle grooves with angles of (**a**) 90° and (**b**) 115° on quartz.

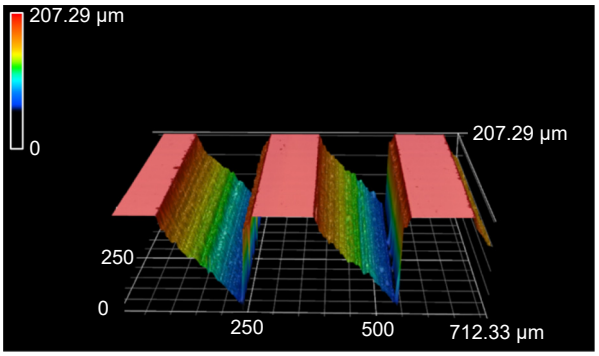

Fig. S7 | Morphology of right-angle triangle grooves on quartz.

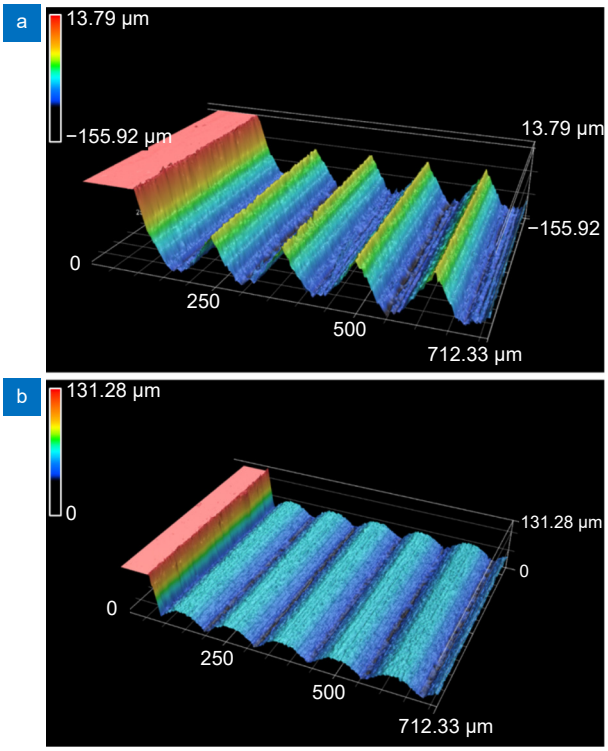

Fig. S8 | Morphology of (**a**) trapezoidal groove array on borosilicate glass, (**b**) cylinder arrays on quartz.

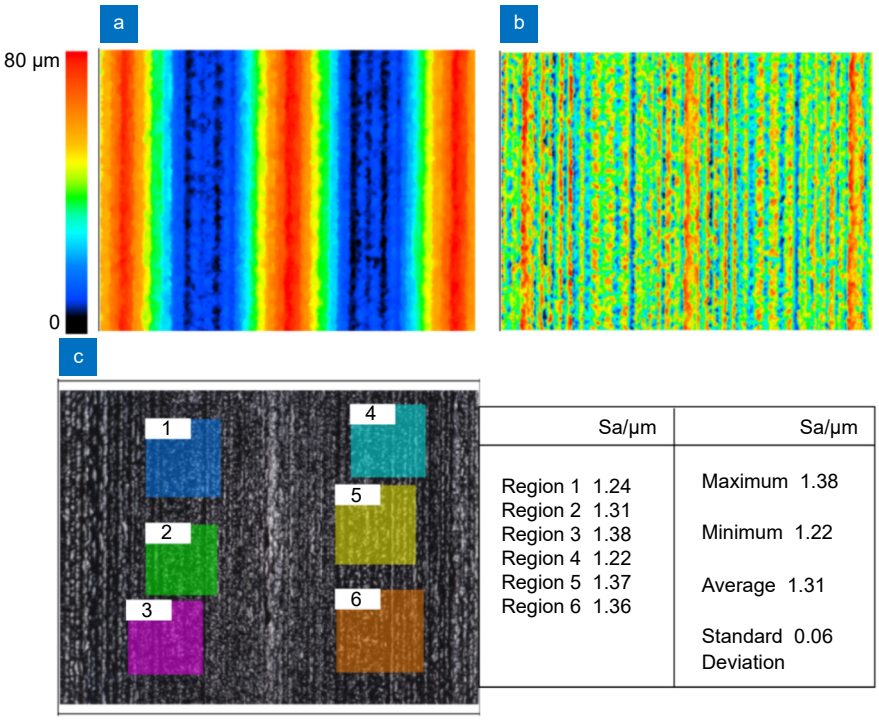

Fig. S9 | Surface roughness detection of trapezoid groove array. (**a**) Raw data. (**b**) Data after removal of surface pattern fluctuation. (**c**) Analysis of surface roughness. The raw data (a) is primarily modulated into a plate (b) with only the removal of the major shape profile. The surface roughness (Sa) is finally obtained by the software analysis.

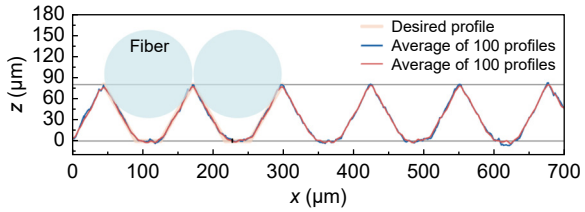

Fig. S10 | Sectional profile of V shape grooves compared to the desired profile, revealing shape error of ~4 μm.

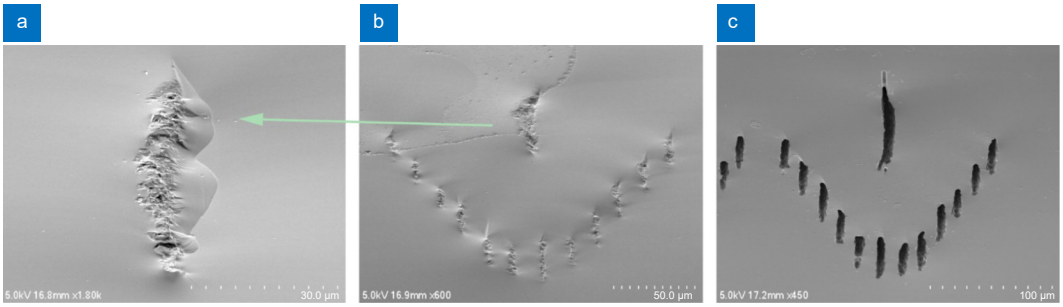

Fig. S11 | 45° tilted view SEM images of laser modulation results with 12-point multi-focus (**a**, **b**) and the result after chemical etching (**c**).

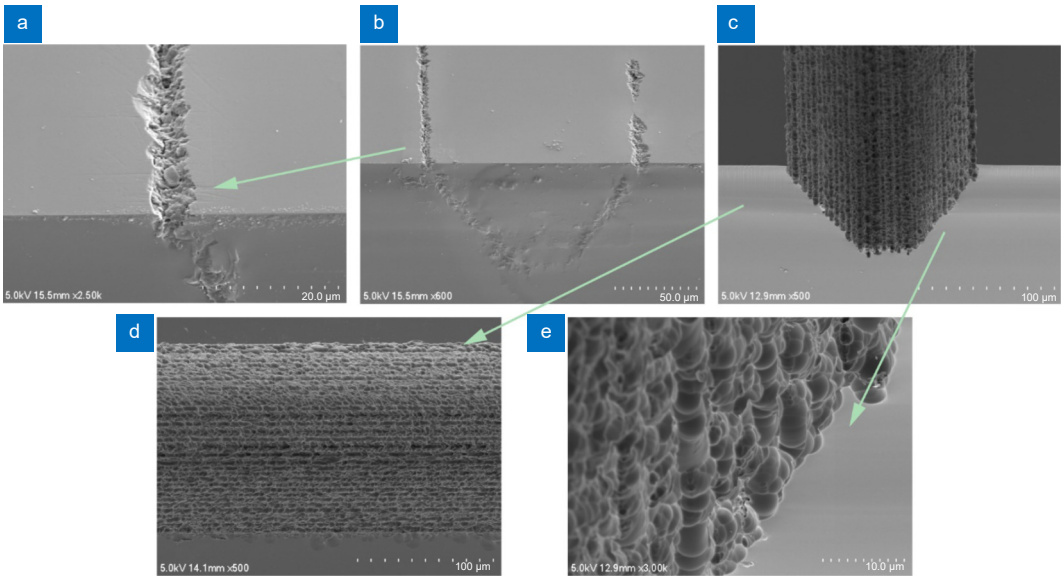

Fig. S12 | 45° tilted view SEM images of laser modulation results with multi-focus forming trapezoidal groove (**a**, **b**) and the result after chemical etching (**c**–**e**). And (d) is the top view.

Section 4: Fabrication parameters for experiments

Table S1 | Fabrication parameters.

Experiments	Materials	Pulse energy/μJ	Pulse width/ps	NA of objective	Scanning speed/mm·s^{-1}	Etching time/h
Fig. 1(e,f,g), Fig. S11, Fig. S12	Fused silica	140	0.3	0.45	20	3
Fig. 2(b)	Fused silica	50	0.3	0.45	10	/
Fig. 2(c)	Fused silica	30/30/50/80/100 for each layer from the top to bottom	0.3	0.65	10	/
Fig. 3(a)	Fused silica	50	0.3	0.45	10	/
Fig. 3(b,c)	Fused silica	60	0.3	0.45	10	/
Fig. 4(b,c)	Fused silica	50	0.3	0.45	10	/
Fig. 4(b,c)	Fused silica	60	0.3	0.45	10	/
Fig. 5(a,b)	Fused silica	40	0.3	0.45	10	3
Fig. 6(a) left	Fused silica	160	3	0.45	10	3
Fig. 6(a) right	Fused silica	140	3	0.45	15	3
Fig. 6(b)	Fused silica	80	0.3	0.65	10	3.5
Fig. 4(c), S8(e)	Fused silica	120	0.3	0.65	30	6
Fig. 4(d), S8(a)	Borosilicate glass	200	10	0.45	20	5
Fig. S4	Fused silica	30/30/50/50/50/80/80/100 for each layer from the top to bottom	0.3	0.45	10	/
Fig. S6(a,b)	Fused silica	140	3	0.45	10	3
Fig. S7	Fused silica	150	3	0.45	10	3